受入
90-1-440
高工研図書室

EUROPEAN ORGANIZATION FOR NUCLEAR RESEARCH

CERN-EP/89-171
20 December 1989

A Comparison of the Structure Functions F_2 of the Proton and the Neutron from Deep Inelastic Muon Scattering at High Q^2

BCDMS Collaboration

A.C. Benvenuti, D. Bollini, G. Bruni and F.L. Navarria
Dipartimento di Fisica dell'Università and INFN, Bologna, Italy

W. Lohmann[1] and R. Voss
CERN, Geneva, Switzerland

V.I. Genchev[2], V.G. Krivokhizhin, R. Lednicky, S. Nemecek, I.A. Savin, G.I. Smirnov and G. Sultanov[2]
Joint Institute for Nuclear Research, Dubna, USSR

U. Meyer-Berkhout, A. Staude, K.-M. Teichert and C. Zupancic
Sektion Physik der Universität, München, Federal Republic of Germany[3]

A. Milsztajn, A. Ouraou, G. Smadja and M. Virchaux
DPhPE, CEN Saclay, France

Abstract

High statistics data on the structure functions F_2 of the proton and the deuteron measured with the same apparatus in deep inelastic muon scattering are used to study the ratio of structure functions of neutron and proton F_2^n/F_2^p and their difference $F_2^p - F_2^n$. Both measurements are consistent with predictions of the quark-parton model and of QCD.

Submitted to Physics Letters B

---

[1] On leave from the Institut für Hochenergiephysik der AdW der DDR, Berlin-Zeuthen, GDR.

[2] Now at the Institute of Nuclear Research and Nuclear Energy, Bulgarian Academy of Sciences, Sofia, Bulgaria.

[3] Funded in part by the German Federal Minister for Research and Technology (BMFT) under contract number 054MU12P6.

In ref. [1] we have presented a measurement of the deuteron structure function F_2^d from deep inelastic muon scattering at high four-momentum transfer Q^2. In the present paper, we use these data together with our earlier measurement of the proton structure function F_2^p in the same kinematic range [2,3] and with the same apparatus [4] to compare F_2^p to the neutron structure function F_2^n.

The deuteron is a loosely bound nucleus and the neutron and the proton can be considered as quasi-free particles. Therefore, the cross section for deep inelastic scattering on deuterons is approximately equal to the sum of the cross sections for scattering on free protons and neutrons and consequently $F_2^d \approx (F_2^p + F_2^n)/2$. The factor 1/2 in this equation is conventional and accounts for the fact that F_2^d refers to a structure function per nucleon.

To convert the measured F_2^d into a structure function of unbound nucleons, corrections have to be applied to account for the Fermi motion of proton and neutron in the deuteron. Such unsmearing corrections have been computed by various authors for different wave functions of the deuteron. We use here the so-called Paris wave function [5] and the correction procedure of Frankfurt and Strikman [6]. For each data point in x and Q^2, an unsmearing factor S is computed such that

$$F_2^p + F_2^n = 2SF_2^d. \tag{1}$$

S is close to unity except at $x > 0.6$. Other unsmearing procedures [7] give similar corrections except at the highest value of x measured in this experiment. Uncertainties in the unsmearing correction are included in the systematic error.

The ratio F_2^n/F_2^p is then calculated from the experimental data as

$$\frac{F_2^n}{F_2^p} = \frac{2SF_2^d - F_2^p}{F_2^p}. \tag{2}$$

This ratio is shown in Fig. 1 as a function of Q^2 and in bins of x. Within the errors, we observe no significant Q^2 dependence of F_2^n/F_2^p in our data. This is in agreement with expectations from perturbative Quantum Chromodynamics (QCD) which predicts only small differences in the Q^2 evolution

between the proton and the neutron structure functions. We therefore average F_2^n/F_2^p over Q^2 in each bin of x. The result is given in Table 1 and is shown in Fig. 2a. Systematic errors were evaluated by adding the individual systematic errors to F_2^d and F_2^p [1,2] and repeating the calculation of eq. (2). This was done for each contribution to the systematic error in turn and the resulting changes in F_2^n/F_2^p were combined quadratically. Since most of the systematic uncertainties are completely correlated between the hydrogen and the deuterium measurement and thus cancel largely in the structure function ratio, the final systematic error is strongly dominated by a relative cross section normalization uncertainty between the two measurements which we estimate to be 2%.

In the quark-parton model, F_2^n/F_2^p can be expressed as a ratio of distribution functions of quarks inside the nucleon. In the region of large x where the contributions from sea quarks are expected to be negligible, and assuming isospin invariance, it can be expressed as

$$\frac{F_2^n}{F_2^p} = \frac{1+4\frac{d}{u}}{4+\frac{d}{u}} \tag{3}$$

where u and d are the distribution functions of up and down quarks in the proton. F_2^n/F_2^p is thus expected to be bound between 1/4 and 4 at least in the region of large x. The data fall between these quark-parton model bounds over the entire kinematic range of the measurement. They extrapolate to $F_2^n/F_2^p \approx 1$ at $x = 0$ and are compatible with $F_2^n/F_2^p \approx 0.25$, corresponding to $d/u = 0$, at $x = 1$. The measured ratio is well described by a parametrization

$$P(x) = 1 - 1.85x + 2.45x^2 - 2.35x^3 + x^4 \tag{4}$$

which fulfills $P(0) = 1$, $P(1) = 1/4$, and $dP/dx(1) = 0$.

In Fig. 2b, we compare our result to data from the European Muon Collaboration (EMC) [8]; in Fig. 2c, we compare them to preliminary results from the New Muon Collaboration (NMC) [9]. Within the errors, we observe agreement between all muon scattering data which were measured in a similar kinematic range. Also shown in Fig. 2c is a F_2^n/F_2^p ratio which we derived from deep inelastic

electron scattering data from SLAC, using recent results on F_2^p and F_2^d [10]. The SLAC results lie above our data, indicating a sizeable Q^2 dependence of F_2^n/F_2^p over the enlarged kinematic range covered by the electron and muon data. Such a Q^2 dependence is not excluded by our data shown in Fig. 1.

In Fig. 2d, we compare again our data to the preliminary NMC results, correcting both data sets for Fermi motion with the unsmearing method described above. Both measurements fall well into a band of width ± 0.015 around the parametrization of eq. (4). From the excellent agreement between the two experiments and from the small systematic error of the NMC data, we thus conclude that the ratio F_2^n/F_2^p is well described by eq. (4) with an uncertainty of about ± 0.015, except for the region $x > 0.6$ where systematic errors and the unsmearing uncertainty become important.

The structure function $F_2^p - F_2^n$ is calculated as $F_2^p - F_2^n = 2(F_2^p - SF_2^d)$ in bins of x and Q^2. We first discuss $F_2^p - F_2^n$ averaged over Q^2 in each bin of x which is given in Table 2 and Fig. 3. Systematic errors were evaluated in the same way as for F_2^n/F_2^p . In Fig. 3, we also show the corresponding result from the EMC and observe again agreement between the two experiments.

The Gottfried sum rule [11] can be applied to $F_2^p - F_2^n$. Assuming isospin invariance and equal sea quark distributions in the proton and the neutron [12], it predicts

$$\int_0^1 [F_2^p(x) - F_2^n(x)] \frac{dx}{x} = \frac{1}{3}; \tag{5}$$

QCD corrections to this Quark-Parton Model prediction are negligible [13]. This sum rule is difficult to test experimentally since the $1/x$ term leads to a large contribution to the integral from the unmeasured region at small x. The measured part of the integral is

$$\int_{0.06}^{0.8} [F_2^p(x) - F_2^n(x)] \frac{dx}{x} = 0.197 \pm 0.006\,(stat.) \pm 0.036\,(syst.)$$

at $Q^2 = 20$ GeV^2. The contribution from the region $x > 0.8$ is negligible. To estimate the contribu-

tion from the small x region, we assume $F_2^p - F_2^n \propto x^\alpha$ at small x and vary α in the range $0.3 \leq \alpha \leq 0.7$; a value of $\alpha = 0.5$ is expected from Regge behaviour. Under this assumption, the unmeasured part of the integral varies between 0.22 and 0.07 such that our data agree with the prediction of the Gottfried sum rule.

We now turn to the Q^2 dependence of $F_2^p - F_2^n$ which, assuming isospin invariance, is a pure flavour nonsinglet structure function. Scaling violations of flavour nonsinglet structure functions are of particular interest when compared to predictions of perturbative QCD since the gluon distribution does not appear in their QCD evolution equations [14]. They thus depend only on the QCD mass scale parameter Λ and their measurement constitutes, in principle, the best method to unambiguously determine Λ in deep inelastic lepton scattering. In practice, however, such structure functions are always obtained as a small difference of two experimental measurements and are therefore affected by larger statistical uncertainties.

To fit QCD predictions to the measured $F_2^p - F_2^n$, we use the same method which is discussed in refs. [15,16]. Since in the present fit the statistical errors are much larger than in our previous measurements [1,15,16] we do not apply any kinematic cuts but use the full domain of the measurement which is limited by the kinematic range of the deuterium data. The Q^2 range of the fit is thus 8 GeV^2 $\leq Q^2 \leq$ 260 GeV^2 (Fig. 2 of ref. [1]). We find in a next-to-leading order analysis in the $\overline{MS}$ renormalisation scheme, assuming four quark flavours,

$$\Lambda_{\overline{MS}} = 250^{+130}_{-110}(stat.) \pm 90\,(syst.)\,MeV$$

in good agreement with our previous measurements. The measured scaling violations are shown as logarithmic derivatives $d\ln(F_2^p - F_2^n)/d\ln Q^2$ in Fig. 4 and are in good agreement with the QCD prediction for $\Lambda_{\overline{MS}} = 250\,MeV$. This is the first time that significant scaling violations are observed in a measurement of $F_2^p - F_2^n$ at high Q^2.

References

1. BCDMS, A.C. Benvenuti et al., CERN-EP/89-170, submitted to Physics Letters B
2. BCDMS, A.C. Benvenuti et al., Phys. Lett. 223B (1989) 485.
3. A. Ouraou, Thèse, Université Paris XI, 1988.
4. BCDMS, D. Bollini et al., Nucl. Instr. Meth. 204 (1983) 333;
   BCDMS, A.C. Benvenuti et al., Nucl. Instr. Meth. 226 (1984) 330.
5. M. Lacombe et al., Phys. Rev. C21 (1980) 861;
   M. Lacombe et al., Phys. Lett. 101B (1981) 139.
6. L.L. Frankfurt and M.I. Strikman, Nucl. Phys. B184 (1979) 107.
7. See e.g. L.P. Kaptar' et al., JETP Lett. 47 (1988) 509.
8. EMC, J.J. Aubert et al., Nucl. Phys. B293 (1987) 740.
9. J. Nassalski, Proc. Europhysics Conf. on High Energy Physics, Madrid 1989, to be published.
10. L.W. Whitlow et al., Univ. of Rochester Preprint UR-1119 (ER-13065-586), subm. to Europhysics Conf. on High Energy Physics, Madrid, Spain, 1989.
11. K. Gottfried, Phys. Rev. Lett. 18 (1967) 1174.
12. WA25, D. Allasia et al., Phys. Lett. 135B (1984) 231.
13. C. López and F.J. Ynduráin, Nucl. Phys. B183 (1981) 157.
14. G. Altarelli and G. Parisi, Nucl. Phys. B126 (1977) 298.
15. BCDMS, A.C. Benvenuti et al., Phys. Lett. 195B (1987) 97.
16. BCDMS, A.C. Benvenuti et al., Phys. Lett. 223B (1989) 490.

Table Captions

Table 1: Results for F_2^n/F_2^p as a function of x. $<Q^2>$ is the average Q^2 of the data in each x bin. To quantify the Q^2 dependence observed in this ratio, we also give the derivatives $d\ln(F_2^n/F_2^p)/d\ln Q^2$.

Table 2: Results for $F_2^p - F_2^n$ as a function of x.

Table 1

x	$<Q^2>$ (GeV^2)	F_2^n/F_2^p	stat. error	syst. error	$d\ln(F_2^n/F_2^p)/d\ln Q^2$	stat. error	syst. error
0.07	15	0.883	0.020	0.042	−0.148	0.069	0.033
0.10	19	0.827	0.011	0.041	−0.032	0.034	0.029
0.14	24	0.779	0.010	0.039	−0.036	0.031	0.028
0.18	29	0.727	0.009	0.037	0.015	0.027	0.024
0.225	36	0.673	0.008	0.034	−0.030	0.024	0.023
0.275	40	0.634	0.008	0.034	−0.037	0.027	0.023
0.35	46	0.576	0.007	0.033	−0.047	0.022	0.023
0.45	49	0.514	0.009	0.031	−0.026	0.032	0.023
0.55	52	0.401	0.012	0.030	0.056	0.052	0.026
0.65	52	0.321	0.015	0.035	0.030	0.089	0.064
0.75	60	0.326	0.028	0.064	0.129	0.205	0.101

Table 2

x	$<Q^2>$ (GeV^2)	$F_2^p - F_2^n$	stat. error	syst. error
0.07	13	0.0481	0.0086	0.0187
0.10	18	0.0698	0.0046	0.0177
0.14	22	0.0839	0.0040	0.0171
0.18	28	0.0965	0.0033	0.0152
0.225	34	0.1047	0.0028	0.0135
0.275	39	0.1029	0.0025	0.0116
0.35	44	0.0923	0.0016	0.0090
0.45	49	0.0668	0.0014	0.0057
0.55	53	0.0451	0.0010	0.0032
0.65	54	0.0234	0.0006	0.0023
0.75	63	0.0074	0.0004	0.0014

Figure Captions

Fig. 1: F_2^n/F_2^p measured in this experiment as a function of x and Q^2, corrected for Fermi motion. The errors are statistical only. The dotted lines indicate the mean value in each bin of x.

Fig. 2: (a) F_2^n/F_2^p measured in this experiment as a function of x, without and with corrections for Fermi motion. The error bars shown with the data points are statistical only. The systematic errors are indicated by the hatched area. The dashed line shows the parametrization $P(x)$ of eq. (4).

(b) F_2^n/F_2^p measured in this experiment as a function of x and corrected for Fermi motion, compared to data from the EMC Collaboration [8]. The hatched area shows the systematic errors of the EMC data.

(c) F_2^n/F_2^p measured in this experiment as a function of x, compared to data from the NMC Collaboration [9] and from SLAC [10]. The hatched area shows the systematic error of the NMC data; the systematic errors of the SLAC data are not available to us. Data on this figure have not been corrected for Fermi motion.

(d) F_2^n/F_2^p measured in this experiment as a function of x, compared to data from the NMC Collaboration [9]. The data on this figure are corrected for Fermi motion. The dashed lines show the same parametrization as in (a) but increased and decreased by 0.015, respectively.

Fig. 3: $F_2^p - F_2^n$ measured in this experiment as a function of x, compared to data from the EMC Collaboration [8]. The hatched areas show the systematic errors of the two measurements.

Fig. 4: Scaling violations $d\ln(F_2^p - F_2^n)/d\ln Q^2$ measured in this experiment as a function of x. Only statistical errors are shown. The line is a next-to-leading order QCD prediction for a mass scale parameter $\Lambda_{\overline{MS}} = 250\,MeV$.

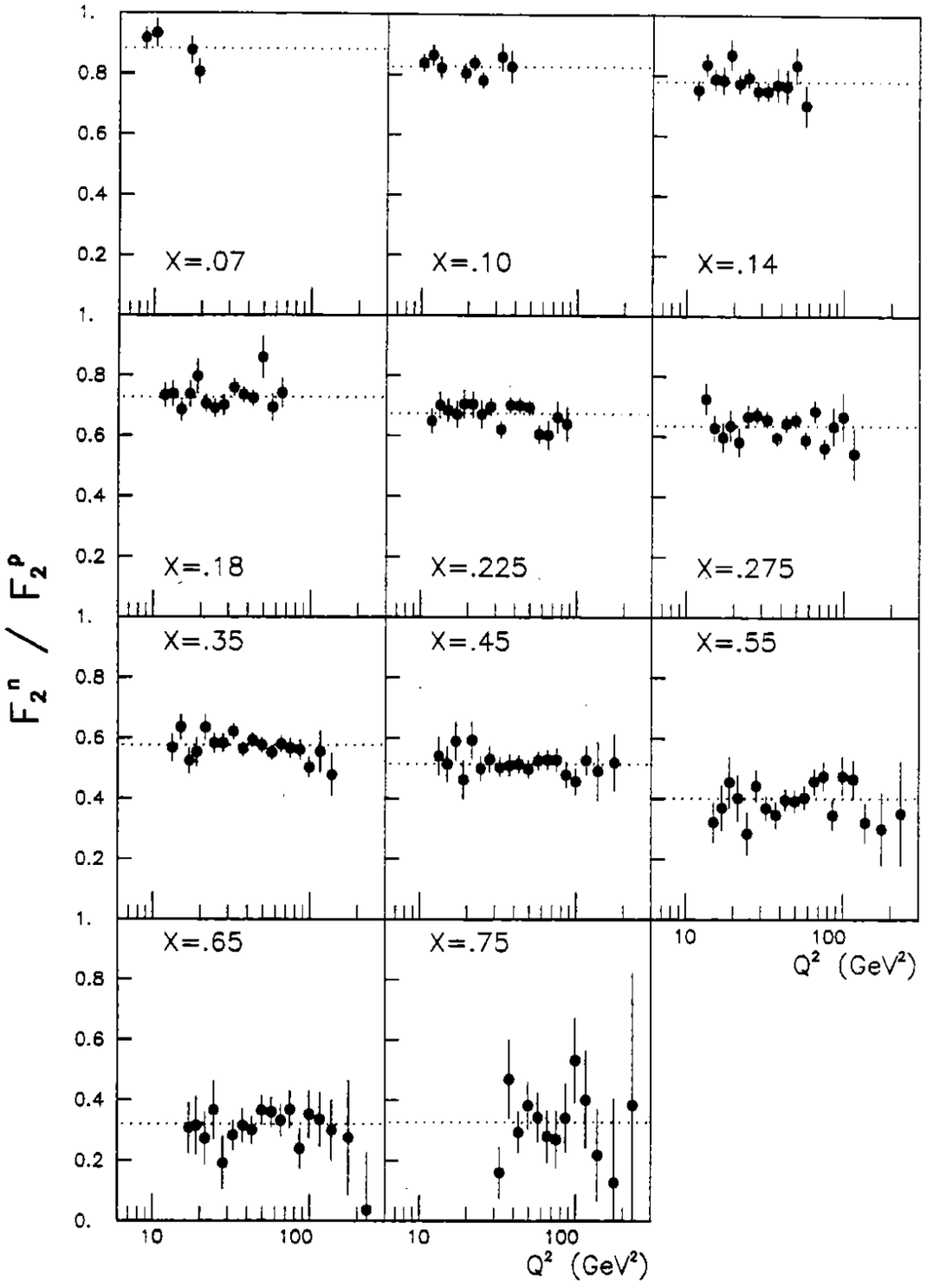
F_2^n / F_2^p
X=.07
X=.10
X=.14
X=.18
X=.225
X=.275
X=.35
X=.45
X=.55
X=.65
X=.75
Q^2 (GeV^2)
Q^2 (GeV^2)

FIG. 1

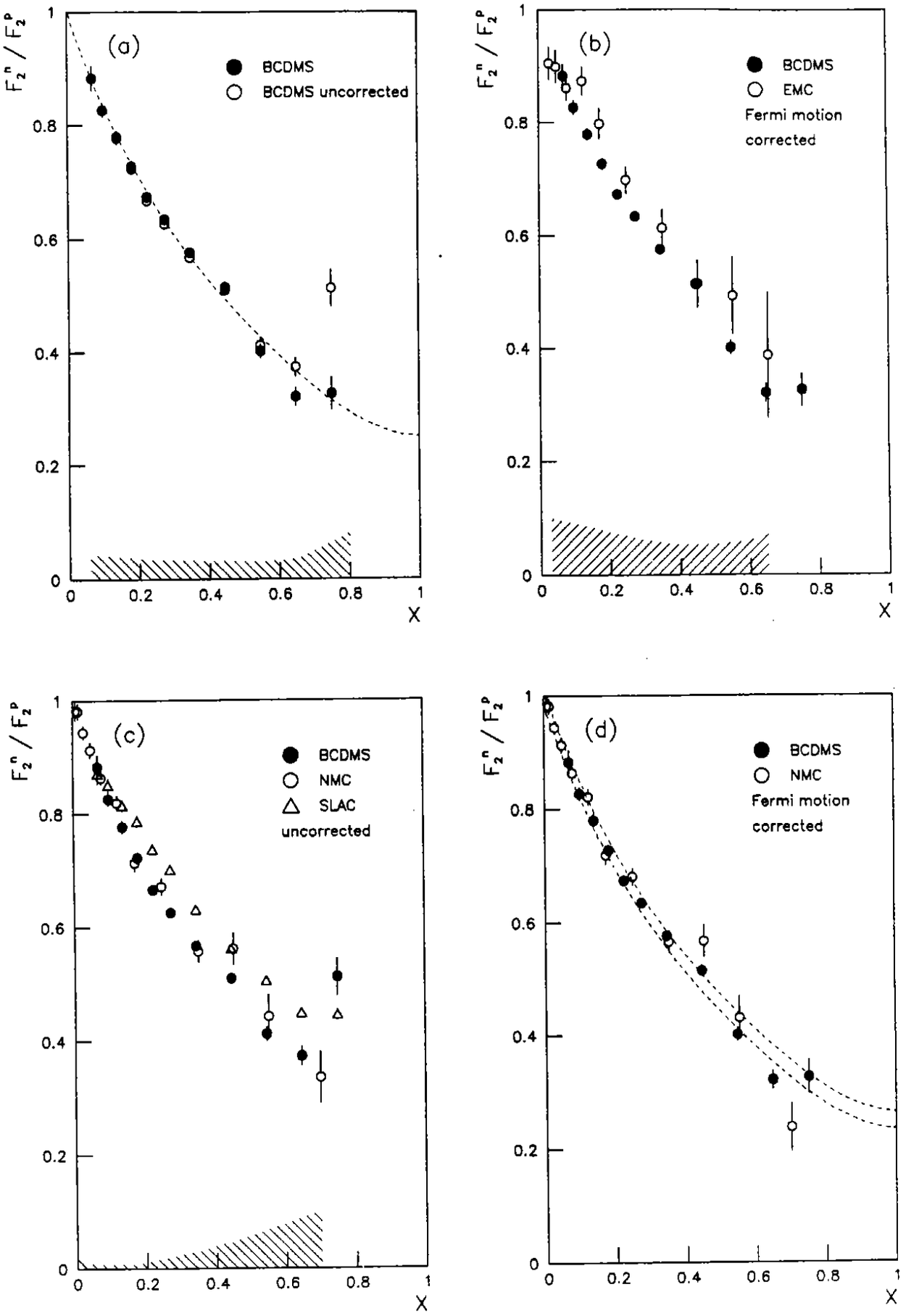
(a)
BCDMS
BCDMS uncorrected
(b)
BCDMS
EMC
Fermi motion
corrected
(c)
BCDMS
NMC
SLAC
uncorrected
(d)
BCDMS
NMC
Fermi motion
corrected
F_2^n / F_2^p
X

FIG. 2

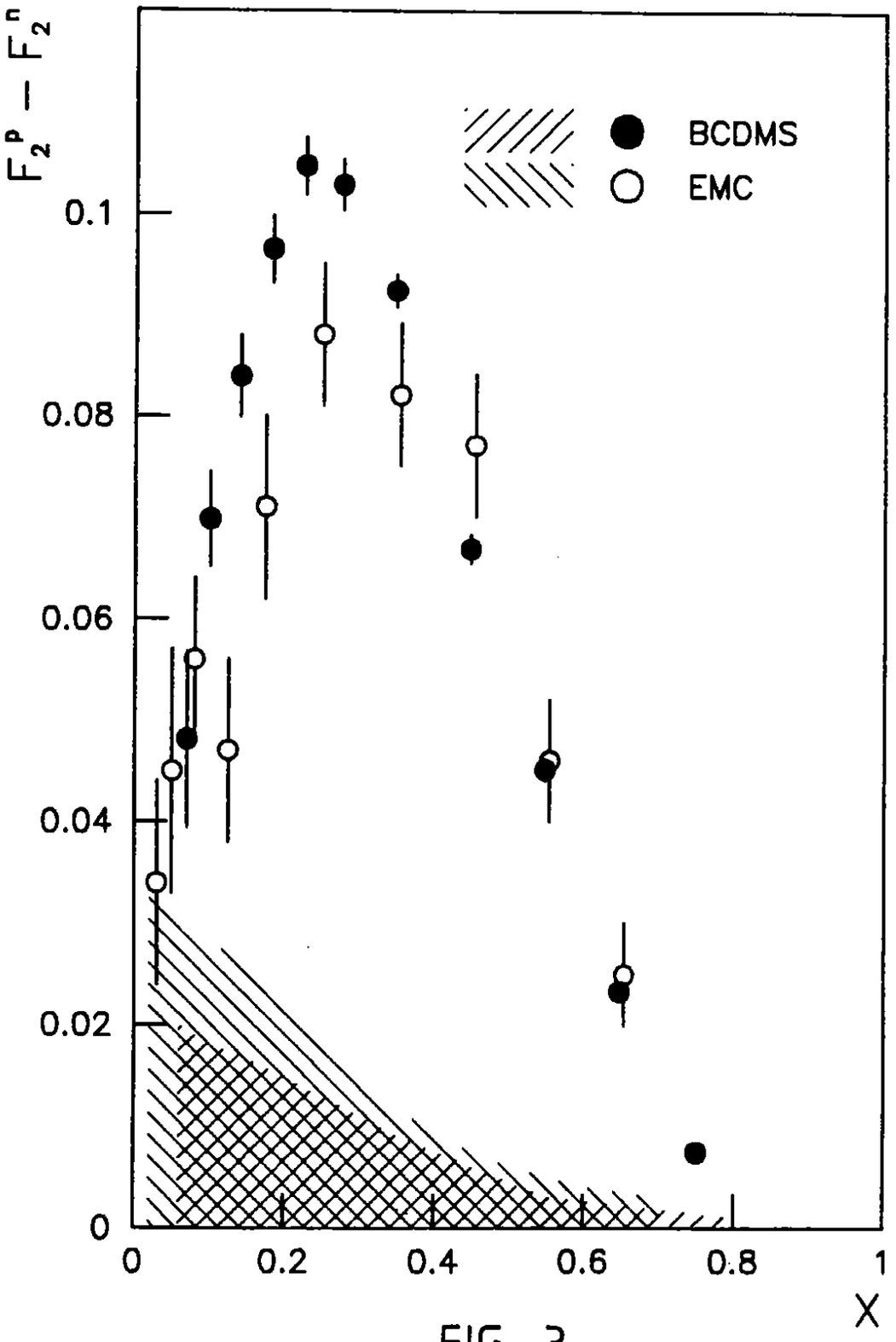

FIG. 3

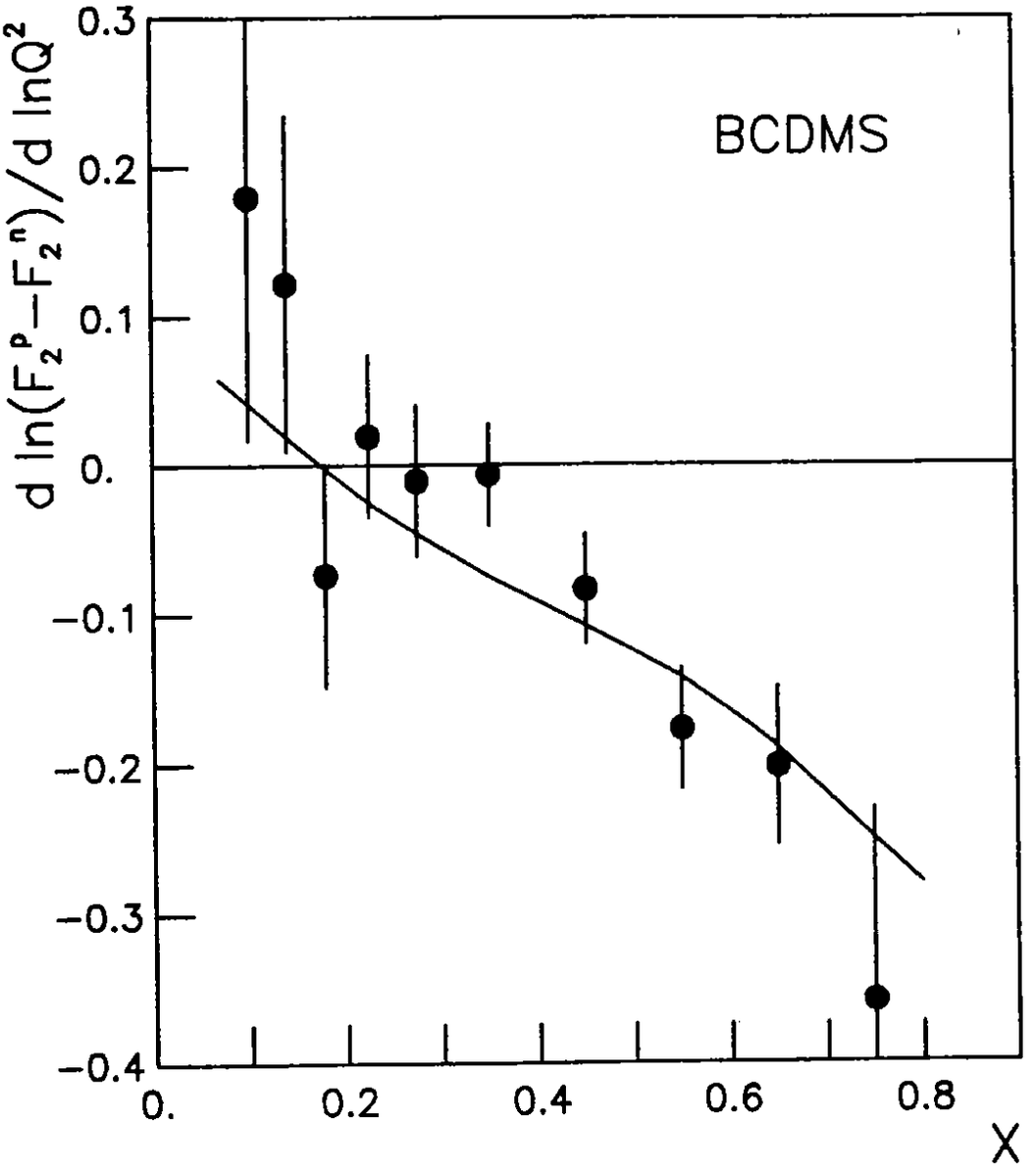

FIG. 4